Laser thermoelasticity of brittle and ductile materials in the initial and modified states

Alexei L. Glazov, Nikita F. Morozov, Kyrill L. Muratikov
glazov.holo@mail.ioffe.ru

Abstract

Non-destructive evaluation of samples made from brittle and ductile materials with various structures with residual stresses was performed by the laser thermoelastic method with piezoelectric signal registration. Main attention was paid to experimental investigations of thermoelastic effect near specially made defects like indentation or holes under external loading. The stress distribution was studied near crack tips, small shallow holes, Vickers indentations and 3D-printed steel samples. It is shown that the laser ultrasonic signal is very sensitive to residual stresses especially in metals. The possible reasons for this signal behavior are discussed and an effect of residual stress on the thermoelastic signal is estimated.

1 Introduction

Laser generation of sound is an important area of modern mechanics and physics of solids [1, 2]. Laser ultrasonic methods also play an increasingly important role in solving problems of non-destructive testing of solids and structures [3, 4, 3, 6]. The basic mechanisms of laser generation of sound in solids are based on thermoelasticity. Important details of laser thermoelasticity depend on the radiation power, the time range of the laser exposure, the type of material [7]. The characteristic times of modern laser sound generation methods ranges from femtoseconds to milliseconds. Materials of various types are being actively studied at present by means of laser thermoelastic methods. Both the time scale and the type of material can impose significant features on thermoelastic processes. Of particular interest are studies that establish specific features of the effects of laser thermoelasticity in materials with a complex rheological structure and containing defects of various types. Attention to these issues is strongly stimulated by the need to develop new methods of nondestructive testing [8, 9].

In this paper, thermoelasticity problems are considered in brittle and ductile materials. The specific feature of this article is that when considering thermoelasticity, pre-stressed state of the material and the presence of plastic deformations in it are taken into account [10]. The main results on laser thermoelasticity were obtained for ceramics as a brittle material [10, 11], and for metals as a plastic material [12, 13, 14]. Near-surface defects in samples is modeled by Vickers and Rockwell

indentations and hole drilling. The laser thermoelastic (TE) signal was measured by a piezoelectric detector. The behavior of laser thermoelastic signals under the action of external unidirectional compressive stress in these materials was studied in details. For ceramics such investigations were carried out for regions near the tips of vertical cracks.

2 Theoretical part

Classical thermoelastic theory is based on two coupled equations, namely, the heat conduction and motion equations. However, for many cases the coupling is small and may be omitted. Then the system of thermoelastic equations may be represented as [15].

$$\nabla^2 T - \frac{1}{\kappa}\dot{T} = -\frac{Q}{\lambda_T}, \tag{1}$$

$$\rho\ddot{\vec{u}} = \mu\nabla^2\vec{u} + (\lambda+\mu)\mathrm{graddiv}\vec{u} - K_\epsilon \mathrm{grad}T, \tag{2}$$

where T is the change of the temperature of the body comparing to the environmental temperature, $\vec{u}$ denotes deformations of the body, Q is the heat produced in the body by external sources, λ and μ are Lam*é* elastic constants, λ_T and κ are the thermal conductivity and diffusivity, K_ϵ is the thermoelastic parameter of the material.

The first equation may be solved independently and the solution is inserted in the equation of motion. The thermoelastic parameter takes place at the equation of motion as well as at the boundary conditions for stresses through the Duhamel-Neiman relation. Because the main aim of the paper is to reveal the relations between the TE signal and the residual stress, we studied a possible stress dependence of elastic parameters.

First of all we will be interested in the dependence of laser ultrasonic signals on mechanical stresses. For this purpose we compare the degree of influence of stresses on the coefficient of thermal expansion and on the mechanical parameters of the material. Let us first consider such dependence for the coefficient of thermoelastic coefficient.

It was shown by thermodynamic methods [16] that in adiabatic conditions and at the independence of PoissonIs ratio on the temperature the thermoelastic parameter is related to the first stress invariant as follows

$$K_\epsilon = K_\epsilon^{(0)} + K_\epsilon^{(1)} = 3K\left(\alpha_T - \frac{1}{E^2}\frac{\partial E}{\partial T}\sigma\right), \tag{3}$$

where α_T is the coefficient of linear thermal expansion, E is Young's modulus, $\sigma = \sigma_{ii}$ is the first stress invariant, K is the bulk modulus, $K_\epsilon^{(0)} = 3K\alpha_T$ is the thermoelastic parameter of a body in the unstressed state.

To get the stress dependence of other elastic parameters one needs to use non-linear elastic theory. Expression for the pressure dependence of the bulk modulus K and

shear modulus μ were obtained in [17]. Coefficients $\frac{dK}{d\sigma}$ and $\frac{d\mu}{d\sigma}$ were derived on the base of non-linear MurnaghanIs model:

$$K(\sigma) = \lambda + \frac{2}{3}\mu - \frac{18l + 2n}{9\lambda + 6\mu}\sigma, \tag{4}$$

$$\mu(\sigma) = \mu - \frac{6m - n + 6\lambda + 6\mu}{6\lambda + 4\mu}\sigma, \tag{5}$$

here λ and μ are Lam*é* constants for the unstressed state, l, m and n are Murnaghan constants. Experiments on the measurement of various sound velocities made it possible to determine the numerical values of $dK/d\sigma$ and $\frac{d\mu}{d\sigma}$ for some materials, and in particular for steel they amounted to $\frac{dK}{d\sigma} = 2.7\pm1.6$ and $\frac{d\mu}{d\sigma} = 6.3\pm1.0$. Note that for other materials these coefficients may be negative.
Scholz and Frankel [18] based on the above approach have estimated the dependence of the Young's modulus and the Poisson's ratio on the uniaxial pressure σ_{11} for steel grade 4340, and obtained the following expressions

$$E = 206.2 \times 10^{-9}(1 - 2.56 \times 10^{-11}\sigma_{11})(\text{Pa}),$$
$$\nu = 0.29(1 - 4.89 \times 10^{9}\sigma_{11}),$$

where σ_{11} is expressed in Pa. Numerical data are obtained on the basis of measurements of sound velocities and subsequent determination of elastic constants of the second and third order (λ=11.04, μ=7.99, l=-38.8±3.6, m=-62.4±2.4, n=-74.7±1.6). That is, these values vary by a few percent near the yield point.
To estimate the influence of the obtained dependences on the TE signal, we consider a simple model of signal generation, which assumes its proportionality to the displacement speed of the sample surface attached to the piezoelectric detector. Let the infinite sample of thickness L be uniformly illuminated by laser radiation, modulated in time according to the harmonic law $I(t) = I_0 \exp(i\omega t)$. Then the time dependent functions will have the form $T(t) = T\exp(i\omega t)$, $u_{xx}(t) = u_{xx}\exp(i\omega t)$, $Q(t) = Q\exp(i\omega t)$, where Q is the thermal flow on the sample surface $x = 0$.
Then, for surface absorption, the temperature is determined from the heat equation

$$\frac{\partial^2 T}{\partial x^2} = \frac{i\omega}{\kappa}T \tag{6}$$

with the boundary conditions

$$K_T \frac{\partial T}{\partial x}\Big|_{x=0} = -Q, T\Big|_{x=L} = 0. \tag{7}$$

The motion equation

$$-\rho\omega^2 u_{xx} = (\lambda + \mu)\frac{\partial^2 u_{xx}}{\partial x^2} - K_\epsilon \frac{\partial T}{\partial x} \tag{8}$$

with the boundary conditions, for instance, for the free surfaces

$$\sigma_{xx}(x = 0) = \sigma_{xx}(x = L) = 0 \tag{9}$$

allows us to calculate u_{xx}. For a thermally thick sample with $L\sqrt{\frac{\omega}{2\kappa}} >> 1$,

$$u_{xx}(L) = 2QK_\epsilon \left(c(\sigma)(K + 4\mu/3) \sin(c(\sigma)L) K_T \sqrt{i\omega/\kappa} \right)^{-1}, \quad (10)$$

where $c(\sigma) = \omega\sqrt{\rho/(K + 4\mu/3)}$. Substituting the above values we get the 4% increase of u_{xx} at σ=1 GPa.

3 Experimental part

3.1 Experimental set-up

All TE images were obtained by scanning laser TE microscope. Thermal and acoustic waves in samples were excited by a solid-state laser radiation at the wavelength 532 nm. The DC laser radiation intensity was periodically temporal modulated by an acousto-optic modulator and focused on the sample surface into a spot of 5 Bxm in diameter. Acoustic waves in a sample were excited at one of the resonant frequencies of a piezoelectric transducer attached to its rear unilluminated side. The PZT detector size was $32 \times 14 \times 7$ mm^3. The operating resonant frequency of the used piezoelectric transducer was near 140 kHz. The voltage from the detector was applied to an input of an amplifier for a piezoelectric signal and then to a lock-in amplifier. The block-schema of the experimental set-up is presented in Fig. 1. Laser TE images were obtained by scanning the sample surface by the laser beam over two coordinates with a 2.5 Bxm step. The known uni-axial compressive mechanical stress was applied during the measurements to the side surfaces of the samples parallel to the illuminated surface.

3.2 Thermoelastic study of cracks in brittle materials

Experimental and theoretical studies of laser TE signals in ceramics near the ends of radial cracks showed the presence of strong peculiarities in their behavior in these regions [10, 11]. Experiments with the external uni-axial stress have demonstrated a strong effect of these stresses on the behavior of laser TE signals near the tips of cracks. By laser photoacoustic microscopy methods the distribution of these features was investigated near the ends of cracks. The analysis of the results obtained in the frequency domain showed that signal formation is primarily due to laser excitation of thermal and thermoelastic waves, and not due to the subsequent generation of acoustic waves.

Experiments with a different orientation of the Vickers indentations in ceramics relative to the direction of the external stress action allowed us to estimate the degree of influence of normal and tangential components of stress on laser TE signals near the tips of radial cracks [19]. It was shown that their behavior corresponds well to the theoretical distribution of normal and tangential stresses near the ends of the surface cracks. Up to a certain magnitude of the indentation load, an increase in the amplitude of the laser signals was observed near the ends of the cracks, which, after reaching it, was saturated. Our experiments on ceramics of silicon nitride and ceramics based on aluminum oxides showed very similar results

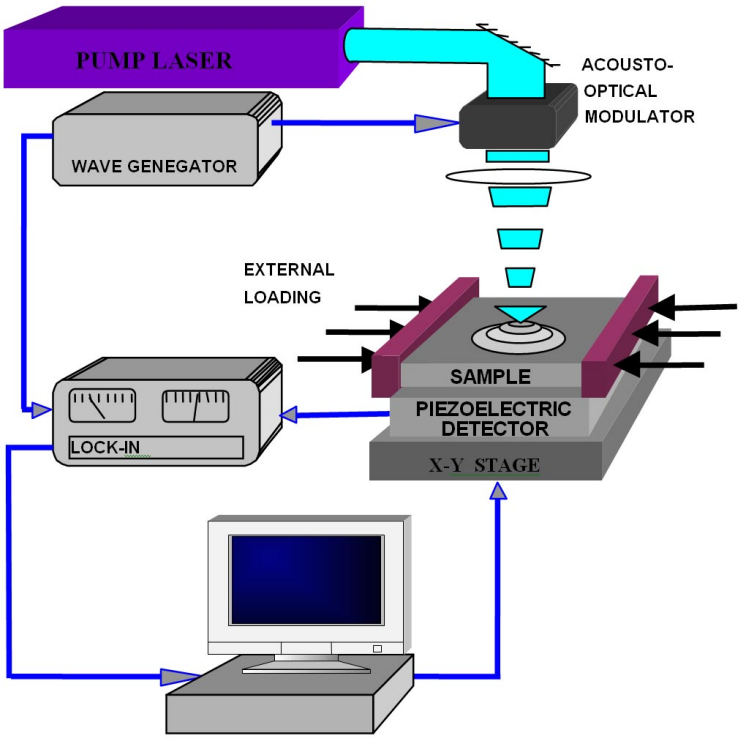

Figure 1: Experimental set-up.

Various ceramics were investigated as brittle materials. The system of cracks was created in the samples by the method of indentation by Vickers. This method allows the reproduction of cracks of a certain length, depending on the load on the indenter. Fig. 2 presents the TE images of the region around the print. On the TE image in the ends of the cracks, a significant increase in the signal is observed. The application of an external uniaxial load at different angles to the cracks made it possible to determine the intensity coefficients.
The stress intensity factors of the crack in general case are determined by the total action of residual stresses and stresses produced by external loading. In linear crack mechanics mechanics the normal and shear components of the total stress intensity factors of a crack can be represented in the form [20]

$$K_I = K_I^{(0)} + K_I^{(1)} \sin^2\phi,\ K_{II} = K_{II}^{(0)} + K_{II}^{(1)} \cos\phi \sin\phi, \tag{11}$$

where $K_I^{(0)}$ and $K_{II}^{(0)}$ are the stress intensity factors which are related to residual stresses, $K_I^{(1)}$ and $K_{II}^{(1)}$ are the stress intensity factors that characterize the crack behavior under external loading, ϕ is the angle between the crack and direction of the external loading.
For small strains near the surface, the change of the TE signal due to the stress may be estimated as

$$\Delta S = AS_0(\sigma_{xx} + \sigma_{yy}), \tag{12}$$

where S_0 is the TE signal from the unstrained sample, constant A depends on the thermoelastic parameters including third-order elastic constants.

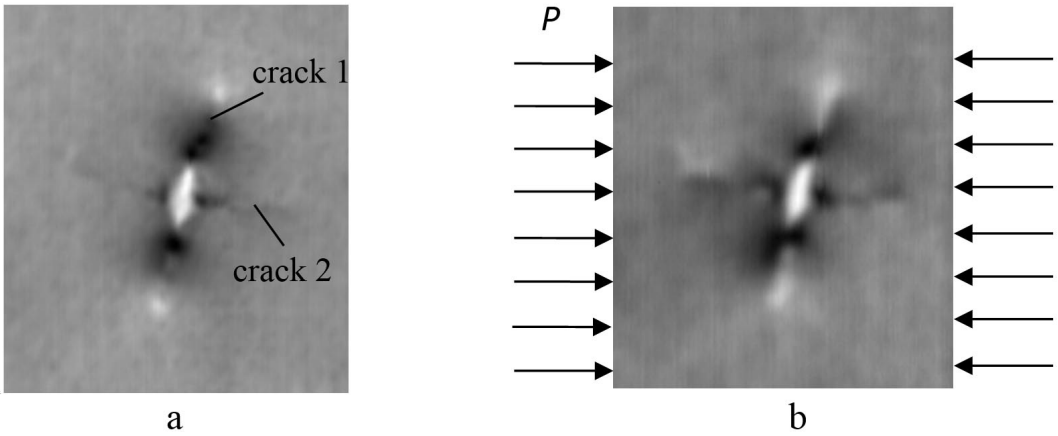

Figure 2: The TE image of Vickers indentation in Al_2O_3-SiC-TiC ceramic a - without external load, b - under the external load of 170 MPa. The indentation load is 98 N, the area is 480×500 μ m^2.

According to [Sedov], the stress tensor components near a crack tip accounting an external loading are

$$\sigma_{xx}+\sigma_{yy}=\sqrt{\frac{2}{\pi r}}\left(K_I\cos\frac{\theta}{2}-K_{II}\sin\frac{\theta}{2}\right), \tag{13}$$

where we used the polar coordinate system with the center at the crack tip.
For residual stress near the tips of radial cracks produced by Vickers indentation with a load P, the stress intensity factors are given by [21]

$$K_I^{(0)}=\chi P/L^{(3/2)},\ K_{II}^{(0)}=0, \tag{14}$$

where χ is a dimensionless factor depending on the crackIs shape and L is the length of the crack.
Then the TE signal near the radial crack tips can be expressed in the form [11]

$$\Delta S=AS_0\sqrt{\frac{2}{\pi r}}\left[\left(K_I^{(0)}+K_I^{(1)}\sin^2\phi\right)cos\frac{\theta}{2}-K_{II}^{(1)}\sin\phi\cos\phi sin\frac{\theta}{2}\right], \tag{15}$$

The detailed analysis of experimental data given in Fig. 2 allows us to estimate ratio $K_I^{(1)}/K_{II}^{(1)}$. For example, the ratio is about 1.4 for crack 1. This result correlates well with a theory of vertical cracks in thick plates [Sedov]. In this case, the theory predicts $K_I^{(1)}=K_{II}^{(1)}$.

3.3 Thermoelastic studies of plastic materials

As a rule, there are no cracks in plastic materials, but many different structures with complex rheology can be formed that contain stress concentrators of various shapes and intensities that can lead to a strong dependence of the TE signal on both internal and external stresses.

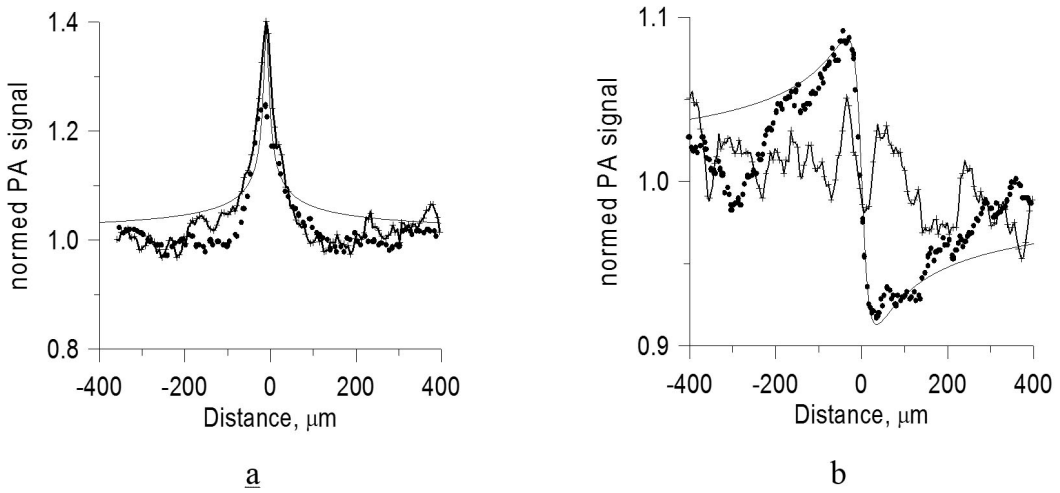

Figure 3: The behavior of the PA signal across the tips of radial cracks. a - for crack 1, b - for crack 2. + denotes the experimental data for the sample without external loading, • denotes the experimental data for the sample under the external loading of 170 MPa, solid line is a theoretical curve.

3.3.1 Method of drilling holes.

The method of drilling holes for the determination of internal stresses is well developed in combination with strain gauges or holographic interferometry [22, 23]. This is primarily determined by the fact that the problem of stress distribution around a small hole in a pre-stressed object was solved quite a long time [8].
The radial and tangential stresses are written as follows

$$\sigma_r = \frac{P}{2}\left(1 - \frac{a^2}{r^2}\right) + \frac{P}{2}\left(1 + \frac{3a^4}{r^4} - \frac{4a^2}{r^2}\right)\cos 2\vartheta, \tag{16}$$

$$\sigma_\vartheta = \frac{P}{2}\left(1 + \frac{a^2}{r^2}\right) - \frac{P}{2}\left(1 + \frac{3a^4}{r^4}\right)\cos \vartheta, \tag{17}$$

where P is the pressure along the axis from which the angle ϑ is measured, a is the radius of the hole, and r is the polar radius. In the case of the formation of the TE signal, we will be interested in the total stress, which in the plane of the surface is equal to

$$\sigma = \sigma_r + \sigma_\vartheta = P - P\frac{2a^2}{r^2}\cos 2\vartheta. \tag{18}$$

Fig.4 demonstrates the graph corresponding to this formula. In mechanics, tensile stresses are positive. However, in our thermoelastic experiments, the TE signal usually increases with compressive stresses, which correlates, for example, with the formula for the coefficient of thermal expansion. When using modulation frequencies in the region of hundreds of kilohertz, the thermal wave length in metallic alloys is of the order of a dozen microns, so even with relatively shallow holes this formula can be considered a good approximation.
A sample for such research was made of a duralumin alloy D16 measuring $6 \times 3 \times 3.6$ mm^3, in the center of which a drill hole of 0.2 mm diameter was drilled at a depth

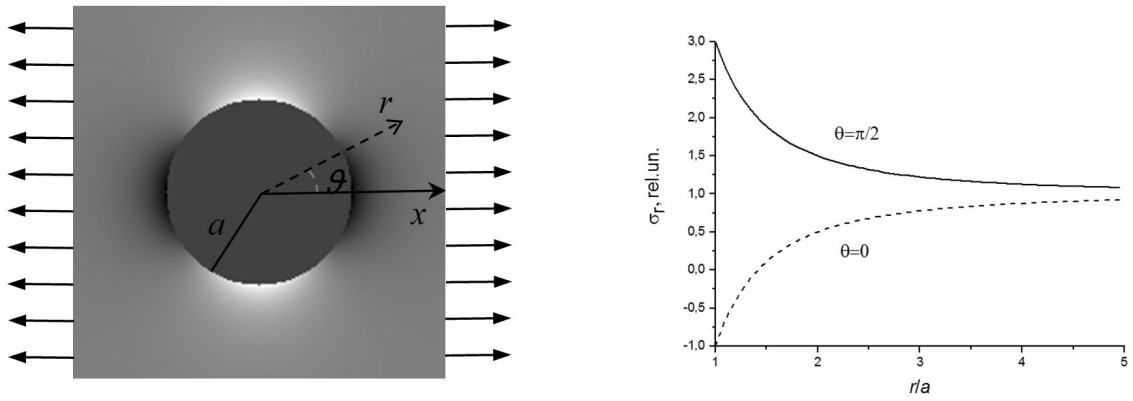

Figure 4: Distribution of stresses around the hole under uniaxial tension P=1.

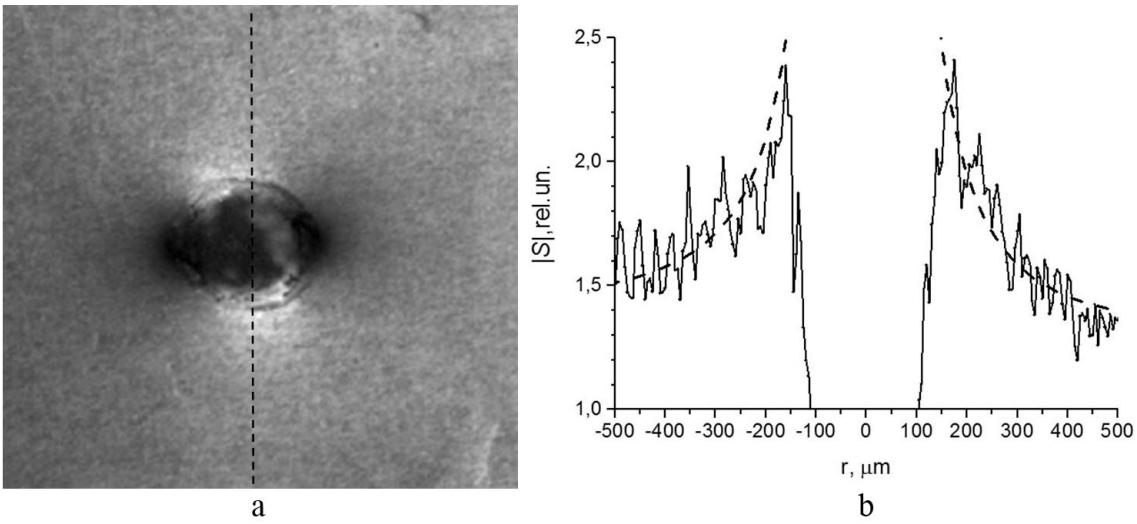

Figure 5: (A) The TE image of a sample from alloy D16 around a small hole. The image size is 1.1×1.1 mm^2. (B) is the cross-section of the TE of the image along the line of the hole through the center at an angle of 90° to the horizontal axis x. The dash curves are the theoretical fitting.

of 0.25 mm. The surface of the sample was previously polished. The TE image of a part of the surface around the hole is shown in Fig. 5. First of all, it should be noted that the length of the thermal wave in the alloy at the used modulation frequency was 15 μm, the effect of the hole on the temperature change did not extend beyond this distance from its edge.

To analyze the behavior of the signal, we have made cross-sections of this image in two perpendicular directions passing through the center of the hole and two circles with a radius of 195 and 225 μm passing in the region of homogeneous heating. A trajectory of the section is shown in Fig. 5 by the dashed line. Minor changes in the signal relative to the trend are reproducible and are determined by the granular structure of the alloy. In accordance with our experimental data, compressive stresses lead to an increase in the signal, and tensile stresses lead to a decrease. In Fig.6 theoretical dependences are also shown in accordance with the Eq.17 for P

= 0.7 and 0.647 for the left and right branches, respectively. It can be seen that although the experimental curves do not have strict symmetry, on the whole they correspond to the theoretical model of stress distribution and, apparently, the TE signal is determined by them entirely. Particular attention should be paid to the strong dependence of the TE signal on internal stresses.
Our further work suggests the study of samples with a calibrated external load.

3.4 Additive technologies

Non-destructive testing of the properties and quality of products obtained with the help of additive technologies becomes more and more relevant in connection with the avalanche expansion of the field of applications and materials. Extremely promising is the use of metal microgranules, which are layer-by-layer sintered. Currently, it is believed that laser ultrasound diagnostics is the most informative and convenient method for these purposes [25].
We used our approach to study samples obtained by 3D printing a steel profile on the surface of a steel plate. As a starting material for printing, a powder from stainless steel 316L was used. The diameter of the initial microgranules was 15/40 μm, and the total thickness of the layer was 3 mm. The general view of the sample is shown in Fig.6a: a homogeneous substrate layer is on the left, a layer obtained by 3D printing is on the right. The image size is 1.5×2 mm^2. The TE image (Fig.6b) demonstrates a strong difference between the signals from the two halves of the sample. In contrast to the substrate, where a sufficiently uniform signal is observed, the change in the normalized signal for the "printed" layer is from 0 to 17. A particularly strong signal increase is observed along the substrate-deposited material boundary. In addition, zones of increased signal around individual grains are observed. In Fig. 6 various images of the border region of the sample are given. Black spots on the optical image are visible open cavities in the material obtained by additive technology. In other places, the heterogeneous structure of the regions seeming to be uniform under the microscope is seen. These inhomogeneities of the TE signal can be caused both by inhomogeneous heating due to the presence of cavities and by the presence of stresses, similar to the distribution of internal stresses arising near the apertures, as was demonstrated in the previous section. When an external load is applied to the TE, the image changes. A characteristic feature of these changes is the decrease in the signal (black regions), mainly around the inhomogeneities elongated along the boundary. This indicates that the residual stresses in these regions were directed across the boundary and, when squeezed in this direction, the total stress decreased. This is consistent with the results of our studies of TE signals around cracks in brittle materials.
For clarity of signal distribution Fig.7 presents a cross section of the TE image along the lines shown in Fig. 6 by the dotted lines. The cross section demonstrates homogeneous behavior at $x < 0$ and very strong signal changes on the right side. Near the border, there are places where the TE signal in 17 times more than that for the homogeneous part. This signal may be reduced by applying pressure perpendicular to the border. Other places, e.g., at x=800 μm, demonstrate strong enhance of the signal, which corresponds to a defect concentrating stress.

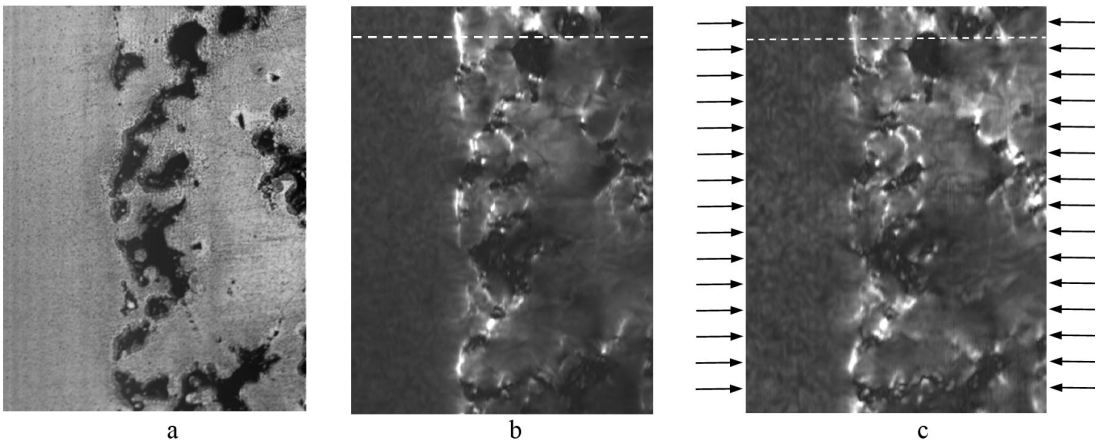

Figure 6: Images of the border region of the sample made of steel with a size of 1.5×2 mm^2. (A) is the optical image, (b) is the TE image, (c) is the TE image of the sample at the uniaxial compression 35 MPa.

Thus, laser thermoelastic diagnostics makes it possible to reveal not only the structure of materials obtained by additive technology, but also the distribution of internal stresses, and this can be done in the production process.

3.5 Indentations in metals

As in the case of ceramics, the indentation method is used in plastic materials for hardness testing. However, in this case, the indenter produces only plastic deformations without cracking. At the same time, however, a system of residual stresses is formed, which is stably reproduced. For the interpretation of the behavior of laser TE signals from indents by Vickers and Rockwell, theoretical models were proposed that take into account their complex rheological structure. Investigation of laser dynamic processes involving thermal, thermoelastic and mechanical processes in such structures are of great interest [26, 27]. Experimentally we found that laser signals have significantly more pronounced features for Vickers indents. We showed by the TE microscopy method that the stress distribution after removing the load on the indenter depends on the state of the sample before indenting [12, 13, 14]. Moreover, the external load can significantly change the stress distribution in the imprint area. Depending on the orientation of the print with respect to the direction of action of the external load, the change in the stress distribution can be reversible or irreversible with the same load. As an example, Fig.8 presents the TE images of Vickers prints in steel in the initial state and under the influence of an external load. The TE signal changes strongly under the load 24 MPa and returns mainly to the initial state after the load relief. This shows that the load has produced elastic effect on the sample and the signal changes were due to the stresses rather than plastic deformation. Again we see that the signal increase was more than 2 times.

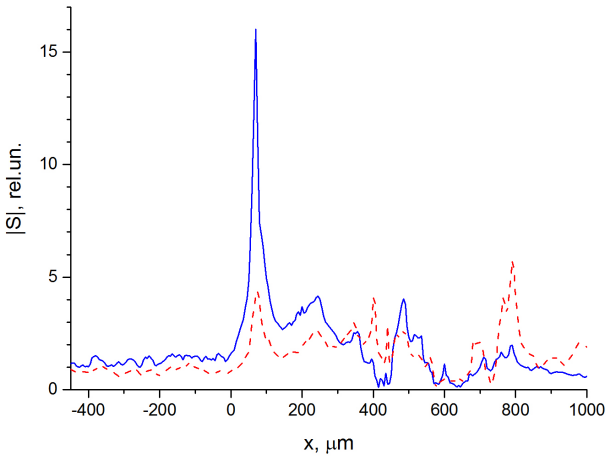

Figure 7: A cross-section of the TE image along the dash line shown in Fig. 7b. Solid blue line is the TE signal for the sample in the initial state, red dash line is the TE signal for the sample under the uniaxial external compressive pressure 35 MPa.

4 Discussion

The study of strained samples from various materials and various inhomogeneities showed a strong dependence on stresses, which is not explained completely by the known dependence of the elastic parameters. At the same time, in brittle materials, the effect of stress on the TE signal was less than in metals. For example, the maximum increase in the TE signal at compressive stresses was about 40% compared to the unstressed state. In metal samples, the excess of the signal from the stressed regions was hundreds of percent. The influence of tensile stresses could suppress the signal practically to zero. The behavior of the signal in cases with a known stress distribution confirms the proportionality of the signal to the first invariant of the stress tensor.

The reasons for an additional increase in the signal in metals can be several. The main reason may be that a two-component model should be used for metals. The main part of the laser radiation is absorbed by the electrons and then is given to the lattice as a result of the electron-phonon interaction. In the general case, to describe such a process, it is necessary to use a two-temperature model that takes into account the electron and lattice temperature difference [28]. Taking into account, however, that the electron-lattice relaxation processes are carried out over times of the order of a few tens of ps, when modulating laser radiation with frequencies in the megahertz range, this difference can be neglected. The classical equations of thermoelasticity take into account the effect of laser excitation of elastic waves only through thermal and thermoelastic phenomena in the crystal lattice. For metals, the contribution of the electronic system to mechanical processes should also be taken into account. As is known, the presence of an electron gas in metals leads to the appearance of a new thermoelastic constant, which takes into account the effect of electrons on lattice deformation. In addition to the dynamic processes in the lattice, conductors in

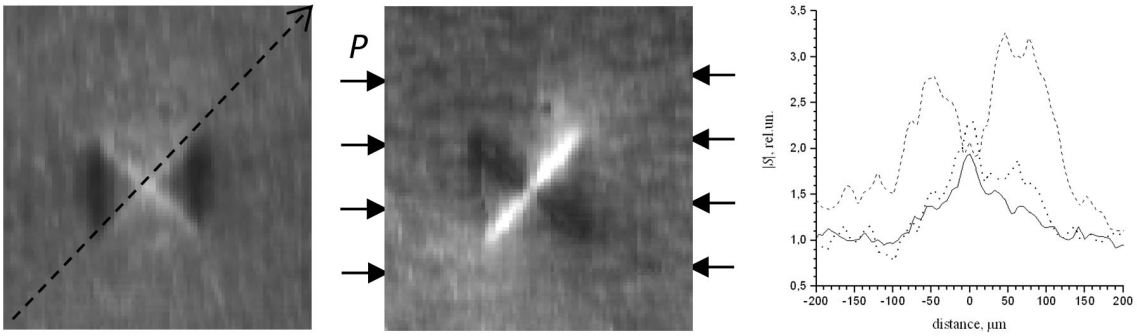

Figure 8: The TE images of Vickers prints in steel grade U8. The load on the indentor is 98N, the image size is 430×430 μm^2. (A) is the sample in the initial state, (b) is the sample under load of 24 MPa, (c) is the TE signal along an indentation diagonal shown as a dash line in (a). The solid, dashed, and dotted curves correspond to the initial sample state, the sample under load, and the sample after load relief, respectively.

parallel have kinematic processes in the electron gas [29, 30]. In the pico-femtosecond range, the interaction of electrons and lattices leads to the effect of an electron shock wave [31]. In the low-frequency range, the absorption of energy by electrons leads to an additional pressure on the lattice, which can lead to an increase in the TE signal.

In the study of imprints from different indenters, a strong change in the TE signal is observed at places of sharp changes in the surface geometry, namely, at the edges of prints and diagonals. These elements are stress concentrators and can lead to an increase in stresses [32] We estimated the stress increase at the diagonals of Vickers indentation up to two orders [13].

In addition, the entire region under the indenter is subject to strong plastic deformation, in which the thermoelastic effect can differ significantly from such an effect in an initial material. First, Young's modulus in the zone of plastic deformation decreases, which, according to Eq. 2, leads to an increase in the influence of stresses on the termoelastic parameter. Secondly, we can talk about nonlinear kinking elasticity observed in solids with plastic anisotropy. These include materials with a layered microstructure and regions with a large number of dislocations. The important mechanical feature of these materials consists in the formation of the stable closed hysteretic loops on their load-displacement curves under cycle loading and unloading. Such a stabilization of the hysteretic loops occurs after several cycles (usually less than 10). It is explained by the formation of reproducible and completely reversible dislocation motion appear in them after several cycles [33, 34, 35]. This circumstance can explain the formation of stable TE signals from the plastically deformed zones of materials during their cyclic laser illumination.

When a certain threshold load is exceeded, reproducible and completely reversible dislocation motion appear in them [33]. These hysteretic loadвГYdisplacement loops can additionally transmit thermal energy into acoustic vibrations.

5 Conclusion

The presented experimental and theoretical results exhibit a strong effect of mechanical stress on the laser TE signals near the tips of cracks in ceramics and from Vickers indented areas in metals. The registered characteristic features of the photoacoustic effect are common for various ceramics and metals subjected to external stress, which goes to show its general nature. The performed analysis has revealed the difficulties of internal and external stress registration by a conventional photoacoustic method that does not use the indentation. In this case, even significant internal or external stresses cause weak changes in the photoacoustic signals generated in metal samples. The presence of stress concentrators significantly enhances the stress influence on the laser TE ultrasonic signal.

Acknowledgments

This work was supported by Russian Science Foundation, project no. 15-19-001892.

References

[1] D. Cerniglia, A. Pantano, C. Mineo, Applied Physics: A, vol.105, pp.959-967, 2011.

[2] T.C. Truong, A.D. Abetew, J.-R. Lee, J.-B. Ihn, ASME J. Nondestructive Evaluation, vol.1, p.021001 (6 pages), 2017.

[3] D. Cerniglia, M. Scafidi, A. Pantano, J. Rudlin, Ultrasonics, vol.62, pp.292-298, 2015.

[4] D. Levesque, C. Bescond, M. Lord, X. Cao, P. Wanjara, J.-P. Monchalin, AIP Conf. Proc., vol.1706, p.130003, 2016.

[5] D. Cerniglia, N. Montinaro, Procedia Structural Integrity, pp.154-162, 2018.

[6] S. Everton, P. Dickens, C. Tdutton, The Journal of the Minerals, Metals (JOM), vol.70, pp.378-383, 2018.

[7] A. C. Tam, Rev. Mod. Phys., vol.58, pp.381-431, 1986.

[8] H. Huan, A. Mandelis, L. Liu, A. Melnikov, NDT&E International, vol.84, pp.47-53, 2016.

[9] H. Huan, A. Mandelis, L. Liu, Int. J. Thermophys., vol.39, pp.39-55, 2018.

[10] K.L.Muratikov, A.L.Glazov, D.N.Rose, and J.E.Dumar, J. Appl. Phys., vol.88, pp.2948-2955, 2000.

[11] K.L. Muratikov, A.L. Glazov, D.N. Rose and J.E. Dumar. Rev. Sci. Instrum., vol.74, pp.3531-3535, 2003.

[12] A.L. Glazov, N.F. Morozov, K.L. Muratikov, Tech. Phys. Lett., vol.42, pp.67-70, 2016.

[13] A.L. Glazov, N.F. Morozov, K.L. Muratikov, Phys. Solid State, vol.58, pp.1735-1743, 2016.

[14] A.L. Glazov, N.F. Morozov, K.L. Muratikov, Int. J. Thermophys, vol.38, p.113, (13 pages) 2017.

[15] L.D. Landau and E.M. Lifshitz. Theory of Elasticity, 187 p., Pergamon, New York (1986).

[16] A.K. Wong, R. Jones and J.G. Sparrow, J. Phys. Chem. Solids, vol.48, pp.749-753, 1987.

[17] D.S. Hughes and J. L. Kelly , Phys Rew., vol.92, pp.1145-1149, 1953.

[18] W. Scholz and J. Frankel, Technical report ARCCB-TR-86004, vol.46, 8 p., 1986.

[19] K. L. Muratikov, A. L. Glazov, D. N. Rose, J. E. Dumar, High Temperatures-High Pressures, vol.34, pp.585-590, 2002.

[20] L. M. Sedov, Mechanics of Continuous Medium, vol.1, 528 p., Nauka, Moscow (1994) (in Russian)

[21] S.M. Smith, and R.O. Scattergood, J. Am. Ceram. Soc., vol.75, pp.305-315, 1992.

[22] A.A. Antonov, Weld Prod., vol.30, pp.29-31, 1983.

[23] ASTM Standard E837-01 Standard Test Method for Determining Residual Stresses by the Hole-Drilling Strain-Gage Method, 2001.

[24] S.Timoshenko and J.N.Goodier, Theory of elasticity, 506p., McGrow-Hill book company, Inc. N.Y, (1951)

[25] Zhong Yang Chua1, Il Hyuk Ahn1, Seung Ki Moon, International journal of precision engineering and manufacturing-green technology, vol.4, pp.235-245, 2017.

[26] D. A. Indeitsev, Yu. I. Meshcheryakov, A. Yu. Kuchmin, D. S. Vavilov, Acta Mechanica, vol.226, pp.917-930, 2015.

[27] D. A. Indeitsev, D. Y. Skubov, D. S. Vavilov, Mechanics and Model-Based Control of Advanced Engineering Systems , Springer, Vienna, pp.181-188, 2014.

[28] L. Jiang, H.L. Tsai, J. of Heat Transfer, vol.127, pp.1167-1173, 2005.

[29] M. Cutler, N.F. Mott, Phys. Rev., vol.181, pp.1336-1340, 1969.

[30] A. Eisenbach, T. Havdala, J. Delahaye, T. Grenet, A. Amir, A. Frydman, Phys. Rev. Lett., vol.117, p.116601 (5 pages)., 2016.

[31] D.Y. Tzou, J.K. Chen, J.E. Beram, J. of Thermal Stresses, vol.28, pp.563-594, 2005.

[32] M.P. Savruk, A. Kazberuk, Int. Appl. Mech, vol.43, pp.182-197, 2007.

[33] P. Finkel, A.G. Zhou, S. Basu, O. Yeheskel, M.W. Barsoum, Appl. Phys. Lett., vol.94, p.241904 (3 pages), 2009.

[34] A. G. Zhou, S. Basu, G. Friedman, P. Finkel, O. Yeheskel, M. W. Barsoum, Phys. Rev. B, vol.82, p.094105 (10 pages), 2010.

[35] B. Anasory, M.W. Barsoum, MRS Communications , vol.3, pp.245вГY248, 2013.

Alexei L. Glazov, Ioffe Physical-Technical Institute, Polytekhnicheskaya 26, 124021 St.Peterburg, Russia
Nikita F. Morozov, Institute of Problems of Mechanical Engineering, Bolshoi pr.VO 61,199178 St.Petersburg, Russia
Kyrill L. Muratikov, Ioffe Physical-Technical Institute, Polytekhnicheskaya 26, 124021 St.Peterburg, Russia